J. Water Environ. Nanotechnol., 4(1): 60-66 Winter 2019

ORIGINAL RESEARCH PAPER

Iron-doped TiO_2 Catalysts with Photocatalytic Activity

Mohammad Ghorbanpour[1], Atabak Feizi[2]

[1] Department of Chemical Engineering, University of Mohaghegh Ardabili, Ardabil, Iran

[2] Department of Civil Engineering, University of Mohaghegh Ardabili, Ardabil, Iran

Received: 2018-12-09 Accepted: 2019-01-06 Published: 2019-02-01

ABSTRACT

The aim of the present study is to synthesize and characterize Fe-doped TiO_2 nanoparticles prepared by a molten salt method using a solid mixture of TiO_2 powder and $FeCl_3$ precursor. As far as this study is concerned, this is the simplest method that has been reported so far for the synthesis of Fe-doped TiO_2 nanoparticles. Pure TiO_2 nanoparticles and 0.5, 1 and 3 wt% Fe-doped TiO_2 samples were prepared. The prepared nanoparticles were characterized by UV-Vis diffusion reflection spectroscopy (DRS), scanning electron microscopy (SEM), X-ray diffraction (XRD) and Energy-dispersive X-ray spectroscopy (EDX). SEM and XRD analysis of the samples indicated the presence of anatase spherical-shaped TiO_2 particles. The results of EDX study confirmed the presence of Fe in all samples. According to DRS results, the band gap energy of Fe doped TiO_2 nanoparticles decreased with increasing Fe concentration from 3.1 eV for pure TiO_2 to 3.0- 2.80 eV for Fe-doped TiO_2. The photocatalytic activity was also checked. It was found that, the photocatalytic activity of Fe-doped nanoparticles was higher than that of the pure TiO_2. The maximum degradation activity of 69% was obtained at the Fe doping content of 0.5 wt%.

Keywords: *Anatase; Iron-Doped TiO2; Molten Salt Method; Photocatalytic Activity*

How to cite this article

Ghorbanpour M, Feizi A. Iron-doped TiO_2 Catalysts with Photocatalytic Activity. J. Water Environ. Nanotechnol., 2019; 4(1): 60-66. DOI: 10.22090/jwent.2019.01.006

INTRODUCTION

TiO_2 is one of the most promising photocatalysts to treat various environmental pollutants due to its high photocatalytic activity, high thermal and chemical stability and non-toxicity [1,2]. Many organic pollutants such as dyes can be degraded by TiO_2 nanoparticles [3-5]. To use TiO_2 nanoparticles as a photocatalyst, it is necessary to induce them by light irradiation with energy levels higher than their band gap energy. Unfortunately, this induction cannot be done with solar light, which restricts their commercial potential [6]. By doping different elements to the structure of TiO_2 nanoparticles can overcome this restriction. In fact, doping decreases the band gap energy of nanoparticles and suppresses (e^-/h^+) pair recombination by electron/hole trapping [7]. Among the various, the applied dopants, doping with iron results in introducing higher oxygen vacancies in the crystal structure and surface of TiO_2, which improves water adsorption, forms surface -OH groups and promotes photocatalytic activity [8]. Adsorbed iron on the surface of TiO_2 nanoparticles can be served as an electron or hole trapper that enhances the separation of free carriers [1].

The synthesis technique plays an important role in the photocatalytic activity of the TiO_2 nanoparticles [9-11]. Nowadays, different methods are used for synthesizing Fe doped TiO_2 such as sol-gel [11-14], hydrothermal [15-17], wet chemical synthesis [18], thermal hydrolysis [19], Solvothermal [20] and calcination of $FexTiS_2$ [21]. Preparation method and characterization of some Fe-doped TiO_2 photocatalysts are summarized in Table 1. An example is Sood *et al.* who prepared Fe-doped TiO_2 nanoparticles by an ultrasonic assisted hydrothermal method followed by calcination. According to their results, the prepared

* Corresponding Author Email: *Ghorbanpour@uma.ac.ir*

nanoparticles possess small size, high visible light response, enhanced photochemical efficiency and thereby excellent photocatalytic activity for the degradation of para-nitrophenol and methylene blue dye under visible irradiation [15]. Recently, the solid-state molten salt method is developed to prepare different types of nanoparticles such as ZnO, CuO, TiO_2 and Ag [9,22-24]. The solid-state molten salt method is an easy, fast and inexpensive approach to provide pure materials. This article introduced a novel, one-step and easy approach for the synthesis of Fe-doped TiO_2 nanoparticles. This method involved the formation of Fe-doped TiO_2 nanoparticles with anatase phase by calcination of a solid mixture of $FeCl_3$ and TiO_2 powder at 700° C for 1 h.

As far as this study is concerned, the synthesis of Fe-doped TiO_2 via molten salt method has never been reported in the literature. This study is focused on the synthesis of Fe-doped TiO2 nanoparticles by the molten salt method. Various concentrations of Fe ions were implied. Characterization of prepared nanoparticles was done by UV-Vis diffusion reflection spectroscopy (DRS), scanning electron microscopy (SEM), X-ray diffraction (XRD) and Energy-dispersive X-ray spectroscopy (EDX). The photocatalytic activity of the prepared nanoparticles was also checked against methyl orange under visible light irradiation.

EXPERIMENT

$FeCl_3$ and titanium dioxide powder were purchased from Merck Company. Various iron contents were considered for the synthesis of Fe-doped titanium dioxide nanoparticles. First, 0, 0.005, 0.01 and 0.03 g equivalent to 3, 1, 0 and 0.5 wt% of iron chloride and 1 to 2 drops of deionized water were added to crucible to dissolve iron chloride. Then 1 g of titanium dioxide was added to it. After grinding and stirring so that iron chloride would uniformly spread in the mixture, the sample was placed in a furnace at a constant temperature of 700 ± 5 °C in ambient atmosphere. After 60 minutes, the sample was removed from the furnace and after cooling, it was washed with ultrasound until the electrical conductivity of the water remained constant before and after washing. Then it was dried at ambient temperature after filtration. The schematic view of the preparation process is presented in Fig. 1.

The morphology and chemical states of iron-doped anatase TiO_2 were analyzed with scanning electron microscopy (SEM) equipped with Energy-dispersive X-ray spectroscopy (LEO 1430VP, Germany). UV-Vis diffuse reflectance spectroscopy (DRS) was adopted using a spectrophotometer

Table 1. Preparation method and characterization of some Fe-doped TiO_2 photocatalysts

Preparation Method	Source of irradiation	Band gap	Pollutant	Initial concentration (ppm)	Performance (%)	Ref.
Sol-gel	visible	1.45	Methylene Blue	-	99	10
Sol-gel	Visible	2.54	Methylene Blue	10	75	13
Sol-gel	UV	2.84	Dichloromethane	96	90	14
Hydrothermal	Visible	2.82	Methylene Blue	10	95	15
Hydrothermal	Visible	2.5	Malachite Green	5	79	17
Solvothermal	Visible	1.79	Methylene Blue	-	98	20
calcination of $FexTiS_2$	Visible	-	phenol	1.88	78	21

Fig. 1. The schematic of the preparation process of TiO_2 nanoparticles

(Scinco S4100, S. Korea). X-ray diffraction)XRD) analysis was done using a PW 1050 diffractometer (Philips, The Netherlands). Scherer's equation was applied to calculate the average crystalline sizes of the particles as equation (1):

$$D = \frac{k\lambda}{\beta \cos\theta} \quad (1)$$

Where λ is the wavelength of X-ray used, k is a constant (k = 0.9), θ is the Bragg diffraction angle and β is the full-width at the half-maximum (FWHM).

The photocatalytic activity of the prepared Fe-doped TiO_2 nanoparticles was measured by the photodegradation of methyl orange (100 mL, 25 ppm and at pH 7) under 250 W visible light radiation (Osram-Germany) in a photoreactor. The rectangular photoreactor (50 cm long, 50 cm wide and 50 cm depth) was made of MDF. The photocatalyst (0.1 g catalyst/100 mL solution) was first dispersed in 50 mL of methyl orange solution and stirred magnetically in the dark for 15 min to achieve adsorption and desorption equilibrium. Then, the solution was irradiated with a source of visible light placed at 5 cm away from the top surface of the glass container. During the experiments, the water jacket circulation system was used to keep the temperature of the solutions at 298 K. Then, the absorbance of the centrifuged solution (10000 rpm for 20 min) was measured to calculate the photocatalytic activity using the UV–visible spectrophotometer. The photocatalytic activity was calculated by the following equation (2):

$$\text{Degradation (\%)} = \left(\frac{A_0 - A}{A_0}\right) \times 100 \quad (2)$$

Where A_0 represents the initial absorbance of dyes solution and A represents the absorbance of the dye at time t.

Table 2. Composition (% w/w) of pure and Fe doped TiO_2 nanoparticles

	0	0.5	1	3
Oxygen	35.36	40.44	42.26	42.28
Titanium	64.64	59.56	56.81	54.85
Fe	-	-	0.93	2.87
O/Ti	0.55	0.68	0.74	0.77

RESULTS AND DISCUSSIONS

The XRD pattern of pure and Fe-doped TiO_2 nanoparticles was shown in Fig. 2. Interestingly, X-ray structural analysis of these samples only showed the typical peaks of the anatase structure without any detectable peaks related to dopant or other structures. So far, because of the high photocatalytic activity of anatase structure, studies on TiO_2 catalysis are often focused on this structure [23]. These results are inconsistent with studies in which the diffraction peaks correspond to the rutile phase [15]. On the other hand, the XRD pattern of prepared samples, even heavily doped sample i.e. TiO_2 nanoparticles doped with 3 % Fe, did not show any diffraction peaks of iron or iron-related compounds, which indicated the formation of an iron-titanium solid solution. This is due to similar ionic radii of titanium and iron (Ti (0.68 Å) and Fe (0.64 Å)), which results in incorporation of the iron ion into the TiO_2 crystal structure [11]. These effects are slightly different from those provided by other reports. For example, Ganesh *et al.* (2007) prepared Fe-doped TiO_2 powders by co-precipitation method. They reported small quantities of secondary -Fe_2O_3 and $FeTiO_3$ phases in their doped samples [25]. In another study, Zhu *et al.* (2006) identified an -Fe_2O_3 phase in Fe-doped

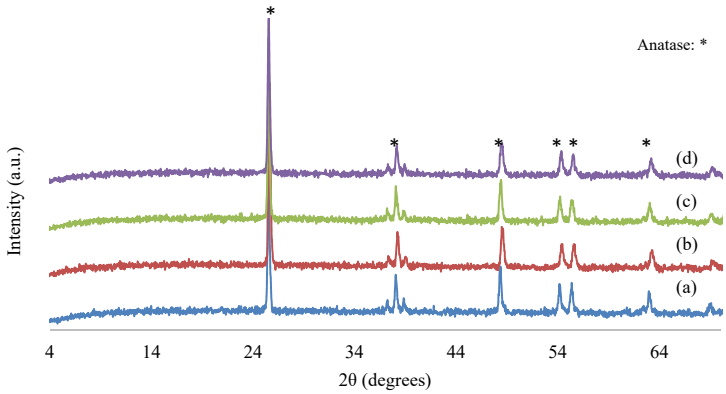

Fig. 2. XRD pattern of TiO_2 nanoparticles (a) doped with 1 (b), 3 (c) and 5 % (d) Fe.

TiO_2 powders prepared by sol-gel [26].

The average crystalline size of the Fe-doped TiO_2 powder was calculated using the Scherrer equation (Table 3). According to this table, crystalline size of the pure TiO_2 nanoparticles was about 53 nm and that of the Fe-doped TiO_2 nanoparticles was in the range of 43.8 to 45.2 nm in diameter. Thus, a major effect of iron doping was the decrease in the anatase-TiO_2 crystalline phase with increasing iron concentration. This result was consistent with the previous studies [11,27]. Therefore, the molten salt method produced Fe-doped TiO_2 powder nanoparticles with dimensions below 50 nm successfully. However, according to previous studies the size of the prepared nanoparticles with other methods was less than 50 nm [27,28]. Nevertheless, it should be noted that the method used in this research was much simpler.

SEM images of the pure and Fe-doped TiO_2 nanoparticles were presented in Fig. 3. This image indicated the spherical shape of pure and Fe-doped TiO_2 particles. Obviously, particle agglomeration happened during synthesizing and drying steps, but redistribution could occur in an ultrasonic bath.

The EDX analysis of pure and Fe-doped TiO_2 nanoparticles was conducted to reveal the presence of iron ions in the structure of the prepared samples (Table 3). Fe ions were detected in 1% and a higher percentage of Fe doped TiO_2 particles. The Fe ions could not be detected in 0.5% Fe doped TiO_2 due to the detection limit of the instrument. According to Table 2, the weight ratio of O to Ti in samples increases with increasing the Fe dopant concentration (0.55 for pure TiO_2 to 0.77 for 3% Fe doped). This variation is because of introducing more oxygen vacancies in the structure of TiO_2 and doping of Fe ions. This observation is consistent with previous studies [29].

UV–Vis spectra of the samples are exhibited in Fig. 4. In the reflection spectra of all doped samples, a shoulder appeared at around 450 nm.

Table 3. The band gap energy of Fe doped TiO_2 nanoparticles

Doping amount (% w/w)	0	0.5	1	3	5
Diameter of the particles (nm)	52.6	44.1	43.8	44.2	45.4
Band gap (eV)	3.2	2.92	2.92	2.8	2.72

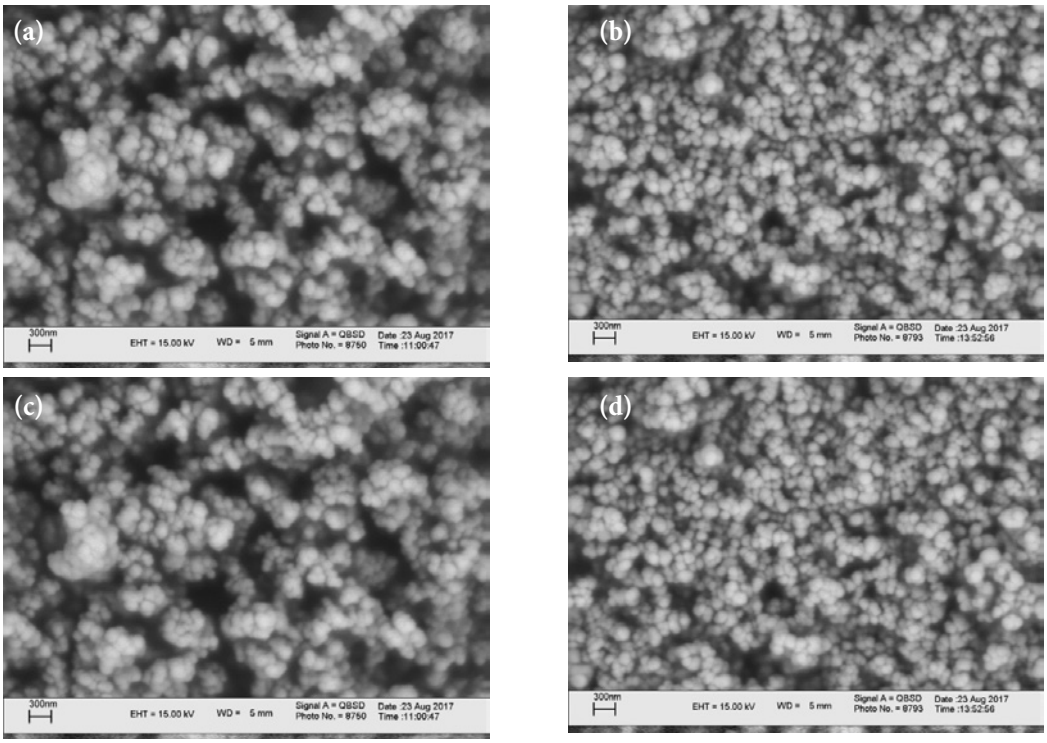

Fig. 3. Typical SEM images of pure TiO_2 nanoparticles (a) doped with 0.5 (b), 1 (c) and 3% (d) Fe

The intensity of this shoulder also increased with increasing dopant concentration. This is due to d–d transition of Fe^{3+} in the TiO_2 structure [30]. Increasing absorption at a wavelength of less than 380 nm (about 3.1 eV) is associated with the intrinsic band gap absorption of pure anatase TiO_2. Doping iron results in absorption in the visible region. These absorptions increase with increasing the iron content due to enhanced visible light absorption. This explains changes in the sample's color from white for pure nanoparticles to yellow or light brown for doped samples. On the other hand, enhancement of absorption in the visible region is related to the excitation of the 3d electrons of Fe^{3+} ions to the conduction band of TiO_2 [15,30].

Fig. 4b showed the Kubelka Munk extrapolation plot i.e. hν versus $(h\nu\alpha)^2$, which was used to calculate band gap degrees of purity and Fe-doped TiO_2 nanoparticles. Where, ν, h and α represent light frequency, Planck constant and absorption coefficient, respectively. The resultant band gap was summarized in Table 3. According to these results, the band gap energy of the doped TiO_2 samples decreases with increasing Fe concentration from 3.1 eV for pure TiO_2 to 3.0, 2.92 and 2.80 eV for 0.5, 1 and 3% Fe doped TiO_2, respectively. Formation of additional electronic states originating from 3d electrons of Fe^{3+} and the interaction between valence band electrons and localized d electrons of Fe^{3+} is the main reason for lowing the band-gap values of doped samples [31]. Accordingly, the photocatalytic activity of TiO_2 is influenced by doping of Fe. In similar studies, Fe-doped TiO_2 particles have band gap energy in the range of 2.45–3.11 eV with a redshift that leads to successful utilization of visible light or solar energy [15,29,30]. For example, the band gap of prepared Fe-doped TiO_2 by Sood et al. was 2.9 eV [15].

The visible light induced the photocatalytic activity of pure and Fe-doped TiO_2 was studied using photocatalytic degradation of methyl orange. The results were presented in Fig. 5. In all of the prepared samples, the concentration of methyl orange decreased rapidly in the first 10 (dark step) min and then decreased slowly (irradiated step). According to Fig. 5, the Fe-doped samples have higher photocatalytic activity than pure TiO_2. The maximum degradation activity of 69 % at 2 h was observed in Fe doped sample with 0.5 wt% Fe. This enhancement of photocatalytic activity caused by doping was in agreement with previous results in the literature [34]. However, in some exceptional

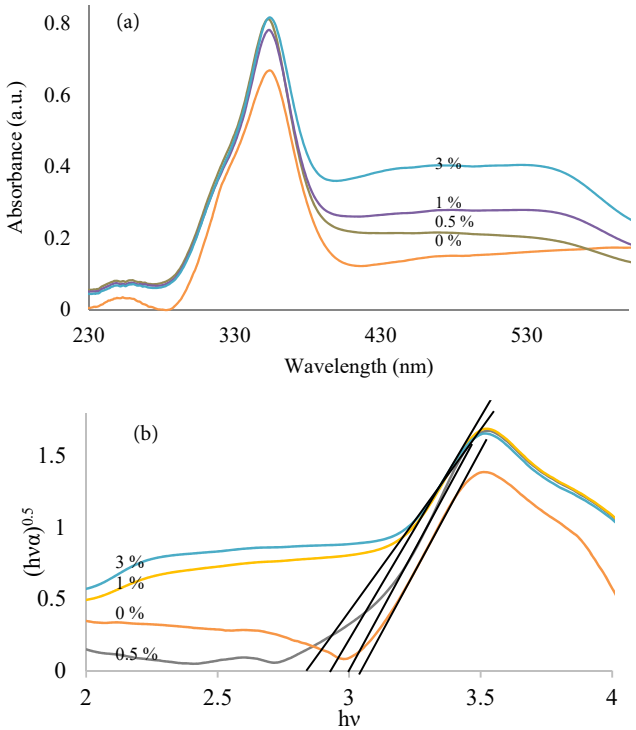

Fig. 4. UV/vis reflectance spectra of TiO_2 nanoparticles (a) and band gap (b) of pure TiO_2 and Fe doped TiO_2 nanoparticles

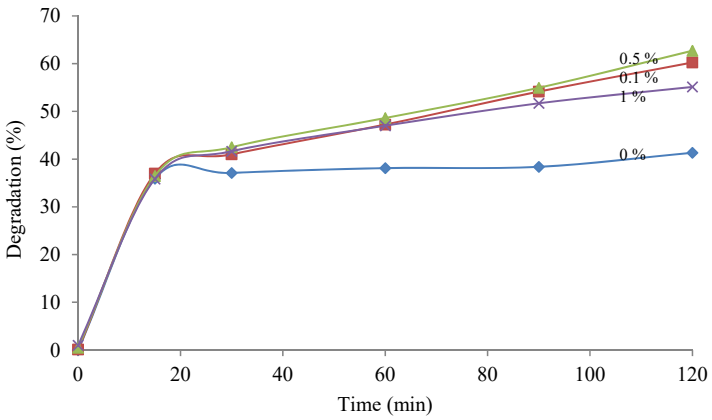

Fig. 5. Photocatalytic activity of Fe doped TiO_2 nanoparticles

cases, the authors did not observe any obvious change after iron doping [30]. It seems that this enhancement arises from the smaller crystalline size and higher light absorption capacity of doped samples than pure nanoparticles (Table 3). Furthermore, the adsorbed Fe on the surface of doped TiO_2 nanoparticles could serve as electrons or holes trapper and enhance the separation of free carriers [1].

According to Fig. 5, if the Fe content is increased further, the photocatalytic behavior of the catalyst will decrease. As discussed earlier, Fe^{3+} ions could serve as electrons and holes trapper. This is due to the reduction of Fe^{3+} to Fe^{2+} through photoelectron capture and oxidation of Fe^{2+} to Fe^{3+} by the O_2 molecules in the media. Therefore, in the presence of small amounts of Fe^{3+}, the electron/hole separation and consequently the photocatalytic activity improved. Nevertheless, when a large amount of Fe^{3+} was doped, the distance between trappers would sharply decline, and Fe^{3+} would turn into recombination centers [33].

Table 1 provides a comparison between the photocatalytic activity of Fe-doped TiO_2 presented by various researchers. By comparing the results of this research with these references, it is observed that the results of the present study are even more acceptable in some cases. It should be noted that the initial dye concentration in the present study is 25 ppm, which is twice more than the value used in the studies presented in Table 1.

CONCLUSION

TiO_2 photocatalysts doped with a different concentration of Fe were synthesized by the molten salt method. Characterization of the prepared samples indicates indicated the formation of spherical pure anatase crystalline structure. The EDX results confirmed the presence of Fe in all of the samples. According to DRS results, the band gap energy of doped TiO_2 samples decreased with increasing Fe concentration from 3.1 eV for pure TiO_2 to 3.02- 2.80 eV for Fe doped TiO_2. Finally, the photocatalytic activity of Fe doped nanoparticles was higher than pure TiO_2. The maximum degradation activity was achieved at the Fe doping content of 0.5 wt%.

CONFLICT OF INTEREST

The authors declare that there are no conflicts of interest regarding the publication of this manuscript.

REFERENCES

1. Crişan M, Răileanu M, Drăgan N, Crişan D, Ianculescu A, Niţoi I, et al. Sol–gel iron-doped TiO2 nanopowders with photocatalytic activity. Applied Catalysis A: General. 2015;504:130-42.
2. TiO2-High Surface Area Materials Based Composite Photocatalytic Nanomaterials for Degradation of Pollutants: A Review. Materials Research Foundations: Materials Research Forum LLC; 2018. p. 48-96.
3. Humayun M, Raziq F, Khan A, Luo W. Modification strategies of TiO2 for potential applications in photocatalysis: a critical review. Green Chemistry Letters and Reviews. 2018;11(2):86-102.
4. Madadi M, Ghorbanpour M, Feizi A. Preparation and characterization of solar light-induced rutile Cu-doped TiO2 photocatalyst by solid-state molten salt method. Desalination and Water Treatment. 2019;145:257-61.
5. Madadi M, Ghorbanpour M, Feizi A. Antibacterial and photocatalytic activity of anatase phase Ag-doped TiO2 nanoparticles. Micro & Nano Letters. 2018;13(11):1590-3.
6. Smirniotis PG, Boningari T, Damma D, Inturi SNR. Single-step rapid aerosol synthesis of N-doped TiO 2 for enhanced visible light photocatalytic activity. Catalysis Communications. 2018;113:1-5.
7. Carneiro JO, Teixeira V, Portinha A, Magalhães A, Coutinho

P, Tavares CJ, et al. Iron-doped photocatalytic TiO2 sputtered coatings on plastics for self-cleaning applications. Materials Science and Engineering: B. 2007;138(2):144-50.
8. Han F, Kambala VSR, Srinivasan M, Rajarathnam D, Naidu R. Tailored titanium dioxide photocatalysts for the degradation of organic dyes in wastewater treatment: A review. Applied Catalysis A: General. 2009;359(1-2):25-40.
9. Ghorbanpour, M., Yousofi, M. and Lotfiman, S., Photocatalytic Decolorization of Methyl Orange by Silica-Supported TiO2 Composites, Journal of Ultrafine Grained and Nanostructured Materials, 50(1), 43-50 (2015).
10. Yadav S, Jaiswar G. Review on Undoped/Doped TiO2Nanomaterial; Synthesis and Photocatalytic and Antimicrobial Activity. Journal of the Chinese Chemical Society. 2016;64(1):103-16.
11. Yeganeh M, Shahtahmasebi N, Kompany A, Karimipour M, Razavi F, Nasralla NHS, et al. The magnetic characterization of Fe doped TiO 2 semiconducting oxide nanoparticles synthesized by sol–gel method. Physica B: Condensed Matter. 2017;511:89-98.
12. Anwar DI, Mulyadi D. Synthesis of Fe-TiO2 Composite as a Photocatalyst for Degradation of Methylene Blue. Procedia Chemistry. 2015;17:49-54.
13. Ali T, Tripathi P, Azam A, Raza W, Ahmed AS, Ahmed A, et al. Photocatalytic performance of Fe-doped TiO2nanoparticles under visible-light irradiation. Materials Research Express. 2017;4(1):015022.
14. Hung W-C, Fu S-H, Tseng J-J, Chu H, Ko T-H. Study on photocatalytic degradation of gaseous dichloromethane using pure and iron ion-doped TiO2 prepared by the sol–gel method. Chemosphere. 2007;66(11):2142-51.
15. Sood S, Umar A, Mehta SK, Kansal SK. Highly effective Fe-doped TiO 2 nanoparticles photocatalysts for visible-light driven photocatalytic degradation of toxic organic compounds. Journal of Colloid and Interface Science. 2015;450:213-23.
16. Alam U, Fleisch M, Kretschmer I, Bahnemann D, Muneer M. One-step hydrothermal synthesis of Bi-TiO2 nanotube/graphene composites: An efficient photocatalyst for spectacular degradation of organic pollutants under visible light irradiation. Applied Catalysis B: Environmental. 2017;218:758-69.
17. Asiltürk M, Sayılkan F, Arpaç E. Effect of Fe3+ ion doping to TiO2 on the photocatalytic degradation of Malachite Green dye under UV and vis-irradiation. Journal of Photochemistry and Photobiology A: Chemistry. 2009;203(1):64-71.
18. Xiang L, Zhao X. Wet-Chemical Preparation of TiO2-Based Composites with Different Morphologies and Photocatalytic Properties. Nanomaterials. 2017;7(10):310.
19. Cui L, Wang Y, Niu M, Chen G, Cheng Y. Synthesis and visible light photocatalysis of Fe-doped TiO2 mesoporous layers deposited on hollow glass microbeads. Journal of Solid State Chemistry. 2009;182(10):2785-90.
20. Wang Q, Jin R, Zhang M, Gao S. Solvothermal preparation of Fe-doped TiO 2 nanotube arrays for enhancement in visible light induced photoelectrochemical performance. Journal of Alloys and Compounds. 2017;690:139-44.
21. Nahar MS, Hasegawa K, Kagaya S. Photocatalytic degradation of phenol by visible light-responsive iron-doped TiO2 and spontaneous sedimentation of the TiO2 particles. Chemosphere. 2006;65(11):1976-82.
22. Lotfiman S, Ghorbanpour M. Antimicrobial activity of ZnO/silica gel nanocomposites prepared by a simple and fast solid-state method. Surface and Coatings Technology. 2017;310:129-33.
23. Bachvarova-Nedelcheva A, Iordanova R, Stoyanova A, Gegova R, Dimitriev Y, Loukanov A. Photocatalytic properties of ZnO/TiO2 powders obtained via combustion gel method. Open Chemistry. 2013;11(3).
24. Ghorbanpour M, Lotfiman S. Solid-state immobilisation of titanium dioxide nanoparticles onto nanoclay. Micro & Nano Letters. 2016;11(11):684-7.
25. Ganesh I, Kumar P, Gupta A, Sekhar P, Radha K, Padmanabham G, et al. Preparation and characterization of Fe-doped TiO2 powders for solar light response and photocatalytic applications. Processing and Application of Ceramics. 2012;6(1):21-36.
26. Zhu S, Liu W, Fan C, Li Y. Mössbauer study of nano-TiO2 doped with Fe. ICAME 2005: Springer Berlin Heidelberg. p. 273-8.
27. Yang X, Cao C, Erickson L, Hohn K, Maghirang R, Klabunde K. Photo-catalytic degradation of Rhodamine B on C-, S-, N-, and Fe-doped TiO2 under visible-light irradiation. Applied Catalysis B: Environmental. 2009;91(3-4):657-62.
28. Wang Q, Xu S, Shen F. Preparation and characterization of TiO2 photocatalysts co-doped with iron (III) and lanthanum for the degradation of organic pollutants. Applied Surface Science. 2011;257(17):7671-7.
29. Abazović ND, Mirenghi L, Janković IA, Bibić N, Šojić DV, Abramović BF, et al. Synthesis and Characterization of Rutile TiO2 Nanopowders Doped with Iron Ions. Nanoscale Research Letters. 2009;4(6):518-25.
30. Adán C, Bahamonde A, Fernández-García M, Martínez-Arias A. Structure and activity of nanosized iron-doped anatase TiO2 catalysts for phenol photocatalytic degradation. Applied Catalysis B: Environmental. 2007;72(1-2):11-7.
31. Yalçın Y, Kılıç M, Çınar Z. Fe+3-doped TiO2: A combined experimental and computational approach to the evaluation of visible light activity. Applied Catalysis B: Environmental. 2010;99(3-4):469-77.
32. Zhang, Z., Wang, C. C., R. Zakaria and Ying, J. Y., Role of particle size in nanocrystalline TiO2-based photocatalysts. The Journal of Chemistry B, 102(52), 10871-10878 (1998).
33. Shi J, Chen G, Zeng G, Chen A, He K, Huang Z, et al. Hydrothermal synthesis of graphene wrapped Fe-doped TiO 2 nanospheres with high photocatalysis performance. Ceramics International. 2018;44(7):7473-80.